Jurnal Ilmu Fisika
Vol. 17, No. 2, September 2025, pp. 146–156
ISSN: 1979-4657 (Print); 2614-7386 (Online)
https://doi.org/10.25077/jif.17.2.146-156.2025

Effect of Cesium Iodide (CsI) Concentration Variation on the Performance of MethylAmmonium Lead Iodide ($MAPbI_3$)-based Perovskite Solar Cells

Shalahuddin Zaki[1], Dahyunir Dahlan[1], Siti Naqiyah Sadiqin[2], Akrajas Ali Umar[2]

[1]Department of Physics, Faculty of Mathematics and Natural Sciences, Universitas Andalas, Padang, 25173, Indonesia.
[2]Institute of Microengineering and Nanoelectronics, Universiti Kebangsaan Malaysia, 43600 UKM Bangi, Selangor, Malaysia.

Article Info

Article History:

Received February 25, 2025
Revised May 26, 2025
Accepted May 29, 2025
Published online June 01, 2025

Keywords:

cesium iodide
device performane
$MAPbI_3$
perovskite

Corresponding Author:

Dahyunir Dahlan,
Email: dahyunir@sci.unand.ac.id

ABSTRACT

The fabrication of $MAPbI_3$ perovskite solar cell (PSC) devices with the modification of adding cesium iodide (CsI) into the PbI_2 layer to enhance performance has been successfully carried out. The used synthesis method was a two-step spin coating with CsI concentration variations: without CsI (control), 2 mg/mL, 3 mg/mL, and 5 mg/mL. Characterization using UV-vis, FESEM, and XRD showed improved in optical properties, morphology, and crystal stability. The UV-Vis spectrum indicated an increase in absorption from 2.29 to 3.17 a.u after CsI addition. FESEM results revealed that a 3 mg/mL CsI concentration produced a uniform morphology, a more compact film layer, and clear grain boundaries compared to other concentrations. XRD analysis showed a 2θ peak shift of 0.04°, indicating changes in crystal lattice parameters and increased lattice density without altering $MAPbI_3$ crystallinity. The device with 3 mg/mL CsI achieved an open-circuit voltage (V_{oc}) of 1.2 V, a short-circuit current density (J_{sc}) of 11.34 mA/cm², a fill factor (FF) of 0.65, a power conversion efficiency (PCE) of 2.8%. In conclusion, 3 mg/mL CsI successfully enhanced PSC performance, but performance declined to 5 mg/mL.

1. INTRODUCTION

Growing global population has led to growing demand for energy. Fossil sources still dominate global energy consumption, but their use has significant environmental impact, such as greenhouse gas emissions and global warming. Renewable energy sources like solar power thus appear as promising alternatives to the problem. Perovskite solar cells are among the most rapidly developed photovoltaic technologies today. In addition to being used in solar panels, perovskite layers can be used in various devices, such as light emission diodes, light detectors, solar fuel cells, and other optoelectronic devices (Roy et al., 2022).

Perovskite solar cells have made significant progress over the past decade, with power conversion efficiency increasing dramatically from 3.8% in 2009 to over 25% in 2023 (Wang et al., 2019). The progress is attributed to their superior optical and electronic properties, including high light absorption coefficients, long charge diffusion lengths, and relatively simple fabrication methods. However, the main challenge that still remains for perovskite solar cells is long-term stability, particularly under high humidity and temperature conditions, which can lead to degradation of the crystalline structure and device

performance (Dewi et al., 2022). One important strategy to enhance the properties of perovskite materials is by doping the MAPbI3 (methylammonium lead iodide) layer. Doping can improve the performance of optoelectronic devices such as solar panels, photodetectors, and light-emitting diodes (LEDs) because it influences the conductivity, photoluminescence efficiency, stability, and other optical properties of the perovskite material (Xiao et al., 2020).

Doping plays a crucial role in reducing the diffusion of unwanted ions, which is one of the primary causes of degradation in perovskite solar cells. By limiting the movement of excess ions, the devices can maintain their performance for a longer period, even in challenging environments such as high humidity and heat exposure. Moreover, doping enhances the energy lattice, which slows down the migration of excess ions within the perovskite material. The reduction of ionic defects, which often act as recombination centers for charge carriers, directly prevents the gradual decrease in the efficiency of the solar cells. As a result, the layer structure becomes more stable and more resistant to degradation caused by exposure to light and oxygen (Habisreutinger et al., 2016).

Based on previous research (Duan et al., 2023), the Cs^+ element in $MAPbI_3$ perovskite produces a consistent spectral shift in the range of 500-760 nm, as well as a longer charge carrier lifetime, which enhances the efficiency of charge collection. Another study (Ašmontas et al., 2022) also found that doping with 10% CsI improves crystal quality, thermal stability, and perovskite efficiency. However, increasing the concentration beyond this point leads to a decrease in thermal stability and efficiency.

Cesium iodide (CsI) is an inorganic compound that improves the performance and stability of perovskite materials by enhancing thermal and phase stability, optimizing crystal structure, and reducing recombination that affects charge transport. As a key precursor in the fabrication of perovskite, CsI helps form a highly stable and efficient structure, making it an essential component in high-performance solar cells. Its use as an interface layer between mesoporous TiO_2 and $MAPbI_3$ significantly increases the energy conversion efficiency from 14.38% to 17.4%. This unique property makes CsI a valuable doping material for developing more stable and efficient perovskite systems such as $MAPbI_3$ components (Han et al., 2017). When CsI is added to the $MAPbI_3$ structure, the doping occurs at sites A and X in the perovskite ABX_3 formula. This study differs from previous research, where CsI intercalation was not used as a precursor but as a doping material that contributes to the growth of perovskite particles and enhances light absorption. The Cs^+ cation replacement partially substitutes the MA^+ site in $MAPbI_3$ structures, thereby improving the structural stability of the perovskite. Therefore, in this study, the synthesis of CsI-doped $MAPbI_3/CH_3NH_3PbI_3$ (MethylAmmonium Lead Iodide) perovskite layers was conducted with varying concentrations of cesium iodide (0 mg/mL, 2 mg/mL, 3 mg/mL, and 5 mg/mL) using a two-step spin-coating method, which showed improved performance (Wang et al., 2021). The addition of CsI to the perovskite layer enhances the quality of the perovskite film by increasing crystal size and reducing defect density, thus improving the efficiency and stability of the devices, which holds potential for further development in perovskite solar cell technology.

2. METHOD

2.1 Preparation of Perovskite Precursors

Lead iodide solution and methylammonium iodide were used as precursors in the deposition of $MAPbI_3$ perovskite. To prepare the lead iodide solution, 600 milligrams of PbI_2, 2 milligrams of MA, and 2 milligrams of HMT were dissolved in 1 milliliter of dimethyl formamide (DMF) and dimethyl sulfoxide (DMSO) at a 9:1 ratio (Umar et al., 2023). The solution was then heated on a hotplate at 110°C while stirring at 700 RPM for four hours. Additionally, the methylammonium iodide (MAI) precursor was prepared by dissolving 60 mg of MAI in 1 ml of isopropyl alcohol and stirring it at 700 RPM for four hours at room temperature. The main solution of phenethyl ammonium iodide (PEAI) was prepared with a high concentration of 6 milligrams (mg) in a scientific solution and diluted using an ultrasonic cleaner for 30 minutes. Next, the P3HT solution was prepared by dissolving 50 milligrams (mg) in 1 milliliter (mL) of chlorobenzene solution. All solutions were filtered before being used in the perovskite fabrication process.

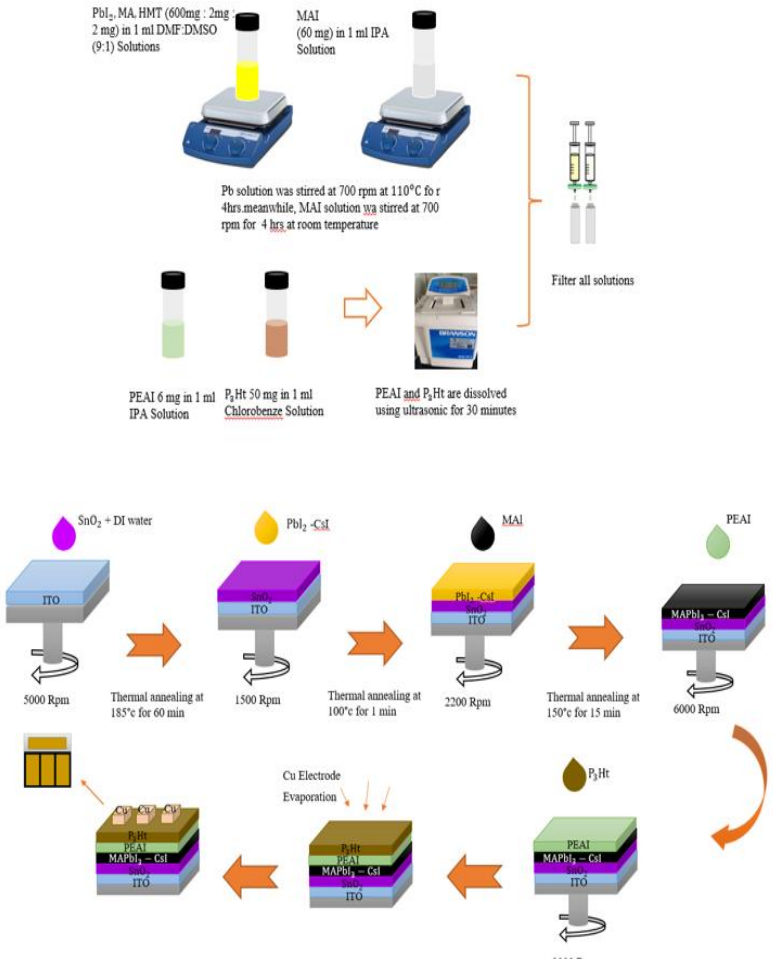

Figure 1. Fabrication process of MAPbI3-CsI-based perovskite device

2.2 Preparation of Perovskite Precursors

The $MAPbI_3$ perovskite layers were fabricated using a two-stage spin coating method on ITO glass substrates. First, 40 µL of PbI_2-CsI solution (concentrations of 0 mg/ml, 2 mg/ml, 3 mg/ml, and 5 mg/ml) was dropped onto an ITO substrate that had been coated with SnO_2. Next, spin coating was performed at 1500 Rpm for 30 seconds. The sample was then heated on a hotplate at 100°C for one minute. After cooling the PbI_2-CsI layer to room temperature, the MAI solution was dynamically deposited onto the PbI_2-CsI layer while the sample was rotated at 2200 Rpm for 30 seconds. Finally, the sample was reheated on a hotplate at 150°C for 15 minutes.

2.3 Characterizations

The morphology and surface shape of the samples were examined using a Zeiss Supra 55VP field emission scanning electron microscope (FE-SEM) (Zeiss, Oberkochen, Germany) at a voltage of 3.0 kV. Furthermore, the crystallinity of the cubic perovskite phase was identified using a Bruker D8 Advance X-ray diffraction (XRD) (Bruker AXS GmbH, Karlsruhe, Germany) with CuKα irradiation (λ = 1.541 Å). To measure the optical absorbance of pure and CsI-doped $MAPbI_3$ perovskite, a Hitachi U-3900H UV-Vis spectrophotometer manufactured in Tokyo, Japan, was used at room temperature with a wavelength range of 300-900 nm. The performance measurements of perovskite solar cells were conducted using a Potentiostat and Newport Oriel Solar Simulator, which were provided by the Institute of Microengineering and Nanoelectronics in Malaysia.

3. RESULTS AND DISCUSSION

3.1 Morphological Characteristics

FE-SEM images of $MAPbI_3$ perovskite with CsI addition show significant changes in surface morphology compared to pure $MAPbI_3$. Pure $MAPbI_3$ exhibits a rough and uneven surface, with protruding grains measuring approximately 400-900 nanometers, surrounded by smaller grains identified as the PbI_2 phase. The average size of these protruding grains is 650 ± 150 nanometers, while the smaller grains have an average size of 100 ± 25 nanometers. These measurements indicate a noticeable difference in surface structure after CsI addition.

The addition of cesium iodide (CsI) has been shown to reduce the formation of smaller PbI_2 grains, improving the grain structure and resulting in a smoother and more uniform surface compared to pure $MAPbI_3$ (see Figure 2C, with labeled areas highlighting the smaller grains). Specifically, at CsI concentrations ranging from 2 mg/mL to 3 mg/mL, the surface morphology closely resembles that of typical $MAPbI_3$ perovskites (Ali Umar et al., 2023). This indicates that CsI incorporation does not alter the fundamental structure of $MAPbI_3$; instead, it enhances surface stability and density by facilitating the formation of smaller and more uniform grains. The uniformity of grain size is confirmed through measurements and visual inspection, with the standard deviation of the smaller grains measured at 60 nm.

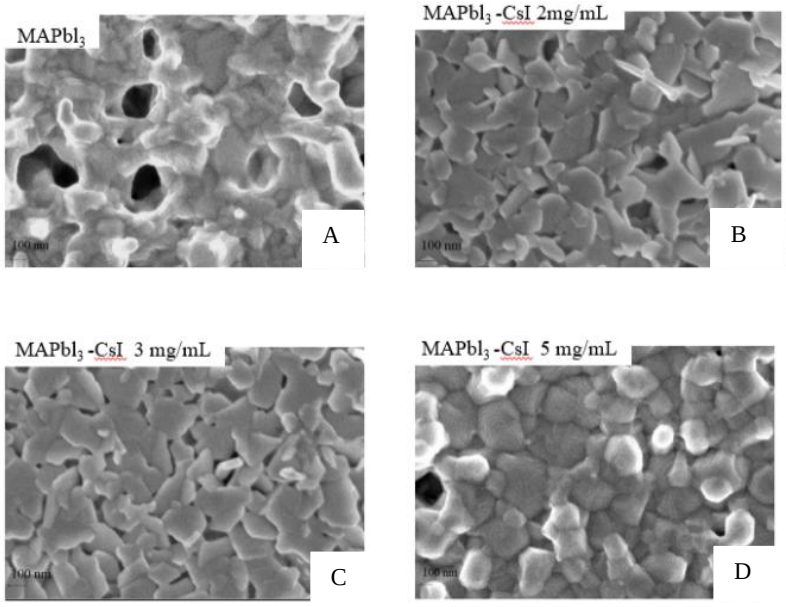

Figure 2. The morphology of pure $MAPbI_3$ perovskite and $MAPbI_3$ with CsI variations at 50.000x magnification

The current findings align with previous studies (Ašmontas et al., 2022), which showed that cesium can alter the surface structure of perovskite. The addition of CsI reduces the size of perovskite grains and creates a more uniform distribution, as CsI acts as a nucleation center to promote crystal growth. This results in more evenly sized grains, with an average size ranging from 100 to 200 nm (Zhang et al., 2018), supported by size dispersion data with a standard deviation of ± 30 nm.

However, at higher CsI concentrations (5.0 mg/mL), a decrease in grain density is observed, along with increased surface roughness and the formation of macro-porous structures, rather than crack-like features, as shown in Figure 2. These results suggest that high concentrations of CsI may disrupt the perovskite structure. According to (Shahiduzzaman et al., 2017), elevated CsI concentrations (corresponding to four Cs^+ double layers) lead to the formation of smaller grains on the surface. These smaller grains are often linked to undesirable phases, such as Cs_4PbI_6, which result from incomplete intercalation and segregation of components during the deposition process.

Overall, the results indicate that CsI can improve the texture and distribution of grains in perovskite up to a certain concentration. However, excessive CsI can disrupt the structure of the perovskite and degrade the quality of the film, potentially reducing its performance in solar cell applications.

3.2 Phase Characteristics

As shown in Figure 3, XRD analysis identified diffraction peaks in the $MAPbI_3$ sample at the (110), (112), (220), and (310) planes. These results indicate that sample P has a cubic perovskite crystal structure of $CH_3NH_3PbI_3$, as recognized from its characteristic diffraction pattern. The diffraction pattern is marked by significant peaks at 2θ angles of 14.08°, 24.4°, 28.24°, and 31.76°. Additionally, the positions of the diffraction peaks observed help identify the crystal planes characteristic of the cubic perovskite crystal system, as indicated by the δ symbol in Figure 3.

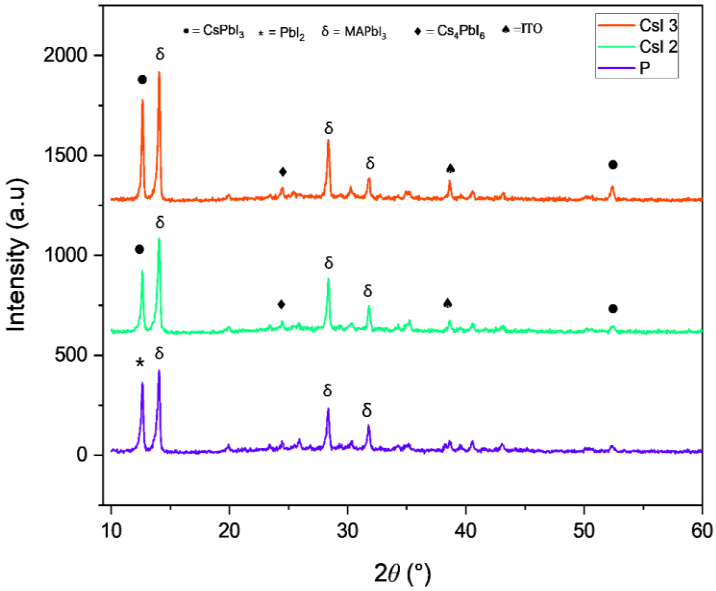

Figure 3. Diffraction patterns of $MAPbI_3$, $MAPbI_3$-CsI 2, and $MAPbI_3$-CsI 3

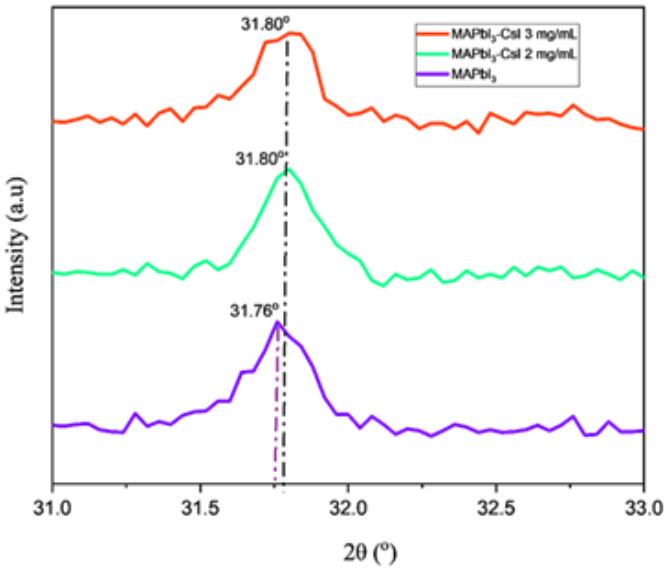

Figure 4. Diffraction patterns of pure $MAPbI_3$ and diffraction patterns of $MAPbI_3$ with the addition of CsI 2 and CsI 3 in the 310 planes.

Figure 3 also reveals the presence of additional peaks, attributed to the PbI_2 layer. The presence of the PbI_2 phase has been previously reported in perovskite films without Cs^+ ions (Ašmontas et al., 2022). This finding is reinforced by the FE-SEM imaging results, which show that perovskite films without Cs^+ contain large grains of approximately 400-900 nm in size, surrounded by smaller grains identified as individual PbI_2 phases. However, after adding 10% CsI to the precursor solution, the presence

of PbI_2 phases was no longer detected. This suggests that the presence of Cs^+ ions is essential for the stability and structure of the perovskite films formed. Cs^+ ions help strengthen the electrostatic interactions between the crystal layers, enhancing the regularity and density of the perovskite crystal structure. Additionally, the presence of Cs^+ ions can influence grain distribution and improve surface morphology, which ultimately enhances the optical and electronic efficiency of the perovskite material. The addition of Cs^+ ions also slows the degradation of the perovskite structure due to environmental factors such as light and oxygen exposure, by improving the material's resistance to these external factors.

The consistency of these findings is demonstrated in Figure 3, which shows that at CsI concentrations ranging from 2 mg/mL to 3 mg/mL, CsI is clearly substituted into the $MAPbI_3$ structure. This is evidenced by the emergence of an additional peak at 12.6°, likely caused by residual PbI_2 formed during the high-temperature annealing process. The intensity of this peak is reduced in the CsI-coated sample, indicating that CsI affects the crystallization mechanism by partially replacing MA molecules with Cs^+ ions. The improvement in crystallization quality of perovskite films by CsI addition has been shown in previous studies (Wang et al., 2021).

The diffraction pattern, which shows the presence of both PbI_2 and the newly identified Cs_4PbI_6 phases, also reveals the appearance of Cs_4PbI_6 at 24°. This finding is consistent with previous research (Shahiduzzaman et al., 2017), which indicates that the presence of Cs_4PbI_6 phases is often associated with the appearance of white particulates on the surface of perovskite layers. These particles can affect the morphology of the coating, potentially leading to structural imperfections and impacting charge transport efficiency in perovskite devices.

The observed shift in diffraction peaks indicates that some of the MA^+ (methylammonium) ions in the $MAPbI_3$ structure have been replaced by Cs^+ ions, which have a smaller ionic radius. This substitution causes a shrinkage of the crystal inter-plane distance, contributing to the shift of diffraction peaks to higher 2θ angles, as shown in Figure 4. This phenomenon is consistent with crystallography principles, where ions with smaller radii replace larger ions in the crystal structure. This contraction not only indicates a change in lattice parameters but also increases the lattice density, which in turn affects the structure and properties of the perovskite material formed.

The presence of Cs^+ ions has been shown to enhance the electrostatic interaction with the $[PbI_6]_4$ octahedral framework in perovskite crystal planes, with the substitution effect being strongest at low concentrations. This effect arises from the smaller radius of Cs^+ ions compared to $CH_3NH_3^+$ ions (MA^+). The effect of Cs^+ ion substitution on structural symmetry has been observed to reach a maximum at a concentration of 3 mg/mL. The enhanced symmetry contributes to maintaining the cubic phase of MAPbI3 (Dahlan et al., 2023), which plays a crucial role in ensuring the structural stability of the material. Therefore, the combination of lattice parameter modification and enhanced symmetry due to CsI doping not only improves the physical and chemical properties of $MAPbI_3$ but also has the potential to enhance the performance and stability of perovskite-based devices (Duan et al., 2023).

3.3 Optical Characteristics

As shown in Figure 5, the optical properties of the $MAPbI_3$ perovskite layer were analyzed by measuring its light absorption using UV-vis spectroscopy. The figure demonstrates an increase in the absorption spectrum around the 600-900 nm range, followed by a decrease, with a peak absorption occurring between 400 and 550 nm. This range falls within the visible light spectrum, which makes up about 40% of the solar radiation that reaches Earth (Austin et al., 2021), highlighting the potential of perovskite technology for efficiently harnessing solar energy.

Figure 5 also reveals that adding CsI to the $MAPbI_3$ perovskite layer improves its absorption ability. In part A of the figure, it can be seen that CsI increases the absorption of the perovskite coating in the 400 to 550 nm range. The absorption value of the pure $MAPbI_3$ sample without CsI is around 1.4-2.29 a.u., while with the addition of CsI at a concentration of 2 mg/mL, the absorption increases to approximately 1.5-2.29 a.u. The absorption further increases to 1.7-3.17 a.u. when a higher concentration of CsI (3 mg/mL) is used.

An increase in absorption indicates that CsI has a significant impact on improving the absorption capacity of the perovskite material, potentially enhancing energy conversion efficiency. The improved light absorption can contribute to better performance in perovskite solar cells. These results are consistent

with earlier research (Ašmontas et al., 2022), which showed absorption values of around 2.0 a.u at 400-550 nm. and are superior to findings from another study (Du et al., 2018) , where adding Cs^+ ions to $MAPbI_3$ single crystals resulted in a maximum absorption at a wavelength of 840 nm at 600-900 nm , remaining stable at around 0.95 a.u. The increase in absorption is beneficial as it can improve the performance of perovskite solar cells by enhancing charge generation and providing better stability than pure $MAPbI_3$.

In Figure 5 (B), the imaging results are shown at a magnified scale. Adding CsI does not shift the absorption edge of the perovskite, as seen in the figure. Instead, CsI incorporation into the $MAPbI_3$ perovskite lattice enhances the interaction of ultraviolet light with the perovskite's electronic system without significantly changing the optical bandgap. This leads to better absorption of ultraviolet light. The findings align with previous research (Han et al., 2017) , which demonstrated that CsI incorporation not only improves absorption at shorter UV wavelengths but also enhances the interface structure, thereby boosting UV resonance efficiency.

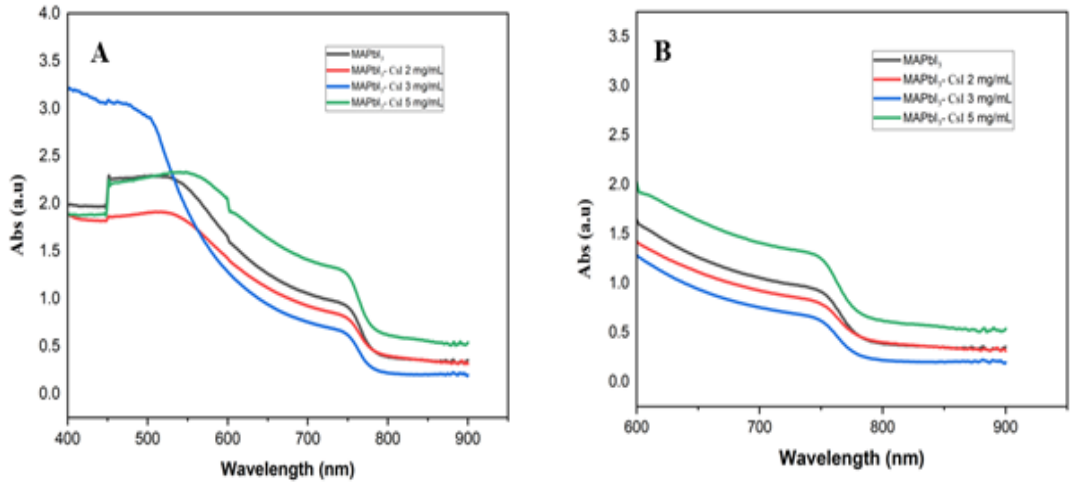

Figure 5. Graph of absorbance spectrum against wavelength (A), Magnification results of UV-vis characterization in the wavelength range of 600-900 nm (B)

3.4 Performance of Perovskite Solar Cells

As shown in Figure 6, the J-V curves illustrate the performance of the $MAPbI_3$ solar cell both without CsI and with varying concentrations of CsI (2 mg/mL, 3 mg/mL, and 5 mg/mL). All curves exhibit a typical J-V curve shape, with broadening observed as CsI concentration increases. Broadening of the curves indicates that the presence of CsI improves both the current and voltage density in the perovskite solar cell, with the optimal performance observed at a concentration of 3 mg/mL..

At the optimal concentration of CsI, the J_{sc} value was measured at 4.8 mA/cm², and the V_{oc} was recorded at 1.2 V. In comparison, the $MAPbI_3$ solar cell without CsI produced a V_{oc} of 0.99 V and J_{sc} of 2.2 mA/cm². The observed lower performance in the sample without CsI is attributed to the predominance of the PbI_2 phase, a non-perovskite phase, which causes increased charge recombination both within the material and at the interface. This phase also results in reduced light absorption within the visible spectrum. Furthermore, the uneven distribution of grain boundaries leads to a direct reduction in both V_{oc} and J_{sc} values (Ašmontas et al., 2022).

As shown in Figure 6, the J-V curves of $MAPbI_3$ and $MAPbI_3$ perovskite devices with different concentrations of CsI (2 mg/mL, 3 mg/mL, and 5 mg/mL) show improved performance with the addition of CsI, especially at a concentration of 3 mg/mL. The addition of CsI at 2 mg/mL increased the open circuit voltage (V_{oc}) to 1.22 V and the short circuit current (J_{sc}) to 10.45 mA/cm². These results suggest that more electrons and holes were successfully collected and transferred to the electrode, indicating that the improvement is due to the more uniform grain distribution, which reduces grain boundary defects. These defects are typically the centers of non-radiative recombination, where charge carriers recombine without generating light. Additionally, the light absorption in the visible spectrum increased, leading to

more photons being converted into free charge carriers, such as electrons and holes (Han et al., 2017).

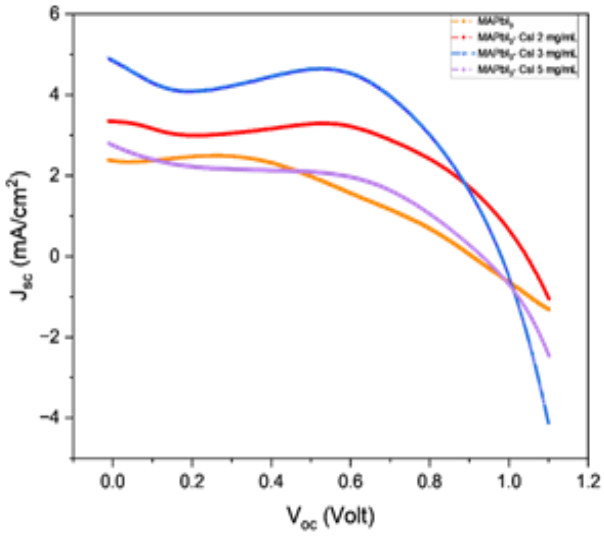

Figure 6. J-V curves of the $MAPbI_3$ perovskite and $MAPbI_3$ with CsI concentrations of 2 mg/mL, 3 mg/mL, and 5 mg/mL.

However, at higher CsI concentrations (5 mg/mL), J_{sc} decreased to 2.75 mA/cm², and V_{oc} decreased to 0.97 V. This decline is attributed to the formation of white granules, identified as the Cs_4PbI_6 phase, which has electronic properties similar to an insulator, thus limiting the material's ability to transport charge carriers effectively (Jiajia Zhang, 2024).

Further confirmation comes from the decrease in the crystal lattice and the formation of structural defects, where excess Cs^+ ions replace $CH_3NH_3^+$ ions in the $MAPbI_3$ lattice. These defects act as charge traps, increasing the likelihood of non-radiative recombination. This phenomenon reduces the number of charge carriers reaching electrodes, which is a key factor in determining the current generation. The impact of these traps is illustrated in Figure 7, where J_{sc}, V_{oc}, fill factor (FF), and power conversion efficiency (PCE) are shown. The data demonstrates a linear increase in these values up to a concentration of 3 mg/mL, followed by a decrease at 5 mg/mL. The incorporation of CsI into MAI and Pb solutions has improved the performance of the devices, as seen by the increase in J_{sc}, V_{oc}, FF, and PCE. In the control device, the maximum FF reached 0.67, with an average of 0.33. In contrast, CsI-modified devices showed maximum FF values ranging from 0.57 to 1.18, with averages ranging from 0.31 to 0.52.

This improvement in performance is consistent with FESEM imaging results, which show that the addition of CsI leads to larger and more compact grains. FESEM measurements confirmed that the grain size for pure $MAPbI_3$ was 800 nm with a standard deviation of 150 nm. However, with CsI concentrations of 2 mg/mL and 3 mg/mL, the average grain size decreased to 500 nm (standard deviation of 100 nm) and 350 nm (standard deviation of 80 nm), respectively. At 5 mg/mL CsI, the grain size increased slightly to 400 nm (standard deviation of 90 nm), but the grain distribution remained much more uniform compared to pure $MAPbI_3$. These results indicate that CsI significantly contributes to improving the grain structure, leading to a more compact and uniform structure, which enhances the material's properties and performance in solar cells.

Furthermore, the UV-Vis characterization results show that the incorporation of CsI increases the light absorption in the perovskite layer, reaching 3.17 a.u. This increase in absorption is beneficial for improving the performance of perovskite solar cells by enhancing the charge generation process and providing better stability compared to pure $MAPbI_3$.

The performance of solar cell devices with different concentrations of CsI is summarized in Table 1. For the pure $MAPbI_3$-based solar cell, the current density (J_{sc}) was 10.79 mA/cm², the open circuit voltage (V_{oc}) was 0.99 V, and the fill factor (FF) was 0.67. These values resulted in power conversion

efficiency (PCE) of 0.99%. However, when CsI was added at a concentration of 3 mg/mL, a significant improvement in device performance was observed. This improvement can be attributed to the positive effect of CsI doping on the perovskite layer.

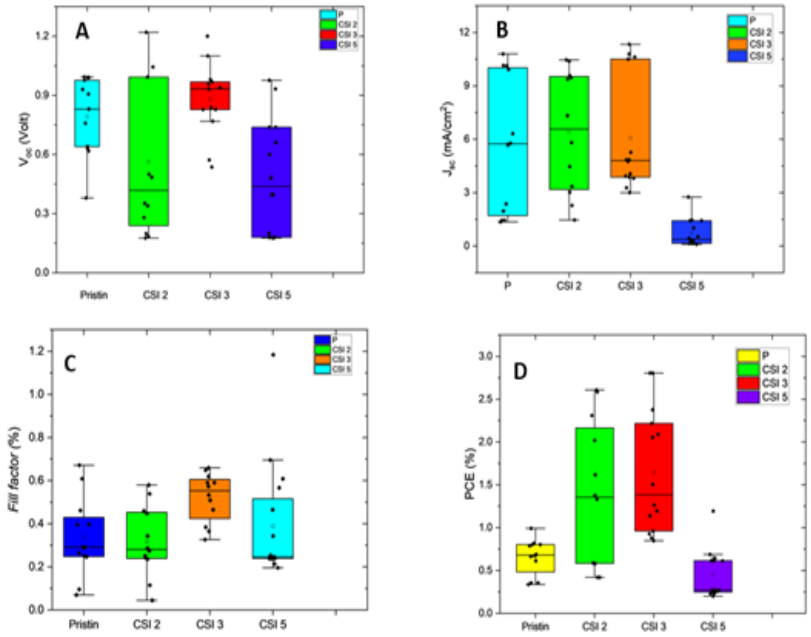

Figure 7. J_{sc} box plot (A), V_{oc} box plot (B), Fill factor box plot (C), and PCE box plot (D).

Despite the improvement, the FF for the pure $MAPbI_3$ sample remains relatively low at 0.67. This indicates that the solar cell's performance is limited by internal losses, such as charge recombination and defects at the grain boundaries. These defects often act as centers for non-radiative recombination, which reduces the efficiency of energy conversion and contributes to low FF. After incorporating CsI, the $_{FF}$ increased slightly to 0.68. This suggests that CsI doping reduces recombination losses by making the grain structure more uniform, improving the overall charge transport. However, the FF still remains below the ideal value of 1, indicating that further optimization of the material and device fabrication is necessary to fully enhance performance.

Table 1. Performance of pure $MAPbI_3$ perovskite and with the addition of various CsI concentrations based on tests from 10 samples.

Sampel	**V_{oc} (V) Max (avg ± sd)**	**J_{sc} (mA/cm^2) Max (avg ± sd)**	**FF Max (avg ± sd)**	**PCE (%) Max (avg ± sd)**
P	0.99 (0.79 ± 0,19)	10.79 (5.6 ± 3.8)	0.67 (0.33 ± 0.18)	0.99 (0.65 ± 0.21)
CsI 2	1.22 (0.56 ± 0.38)	10.45 (6.41 ± 3.40)	0.57 (0.31 ± 0.16)	2.60 (1.37 ± 0.85)
CsI 3	1.2 (0.88 ± 0.18)	11.34 (6.06 ± 3.18)	0.65 (0.52 ± 0.11)	2.80 (1.64 ± 0.72)
CsI 5	0.97 (0,48 ± 0,28)	2.75 (0.75 ± 0.77)	1.18 (0.38 ± 0.26)	1.19 (0.45 ± 0.27)

4. CONCLUSION

The addition of Cesium Iodide (CsI) at an optimal concentration of 3 mg/mL significantly improves the power conversion efficiency (PCE) of MAPbI3-based perovskite solar cells, reaching a maximum efficiency of 2.80%, with an open-circuit voltage (V_{oc}) of 1.2 V and a short-circuit current (J_{sc}) of 11.34 mA/cm². These improvements suggest that CsI enhances the material's structure, increases light absorption, and optimizes the generation of charge carriers (electrons and holes).

However, when CsI concentration exceeds 3 mg/mL (at 5 mg/mL), the performance of the solar cells decreases due to the formation of the Cs_4PbI_6 phase, which acts as an insulating material. This leads to a drop in J_{sc} to 2.75 mA/cm² and V_{oc} to 0.97 V, while also increasing electron-hole recombination and reducing charge transport efficiency.

Therefore, it is crucial to limit the CsI concentration to an optimal level to maintain the stability of the perovskite structure and preserve the efficiency of the device. For future development, further research should focus on optimizing the CsI concentration to improve charge transport and overall solar cell performance. Additionally, refining the deposition process, such as adjusting the film thickness and annealing conditions, could help achieve better fill factors (FF) and enhance device stability. These advancements could lead to more efficient and durable perovskite solar cells, making them viable for future commercial applications.

ACKNOWLEDGEMENT

We acknowledge the financial support from the Universitas Andalas under research grant no. 120/UN16.19/PT.01.03/PSS/2024.

REFERENCE

Ali Umar, M.I., Ahdaliza, A.Z., El-Bahy, S.M., Aliza, N., Sadikin, S.N., Ridwan, J., Ehsan, A.A., Amin, M.A., El-Bahy, Z.M., Ali Umar, A., 2023, Optoelectrical Properties of Hexamine Doped-Methylammonium Lead Iodide Perovskite under Different Grain-Shape Crystallinity, *Nanomaterials*, Vol. 13, DOI: 10.3390/nano13071281.

Ašmontas, S., Čerškus, A., Gradauskas, J., Grigucevičienė, A., Juškėnas, R., Leinartas, K., Lučun, A., Petrauskas, K., Selskis, A., Sužiedėlis, A., Širmulis, E., 2022, Impact of Cesium Concentration on Optoelectronic Properties of Metal Halide Perovskites, *Materials*, Vol. 15, DOI: 10.3390/ma15051936.

Austin, E., Geisler, A.N., Nguyen, J., Kohli, I., Hamzavi, I., Lim, H.W., Jagdeo, J., 2021, Visible light. Part I: Properties and Cutaneous Effects of Visible Light, *Journal of the American Academy of Dermatology*, Vol. 84, Hal. 1219–1231, DOI: 10.1016/j.jaad.2021.02.048.

Dahlan, D., Hardi, A.F., Sadikin, S.N., Umar, M.I.A., Hamzah, A.A., Fauzia, V., Ridwan, J., Maulidiyah, M., Nurdin, M., Umar, A.A., 2023, Improving the Optoelectrical Properties of Humid Stable, Hexamined Perovskite Lattice by Phenetylammonium Cation Additive, *Optical Materials*, Vol. 145, Hal. 1–8, DOI: 10.1016/j.optmat.2023.114489.

Dewi, H.A., Li, J., Erdenebileg, E., Wang, H., De Bastiani, M., De Wolf, S., Mathews, N., Mhaisalkar, S., Bruno, A., 2022, Efficient Bandgap Widening in Co-Evaporated $MAPbI_3$ Perovskite, *Sustainable Energy and Fuels*, Vol. 6, DOI: 10.1039/d1se01692j.

Du, S., Jing, L., Cheng, X., Yuan, Y., Ding, J., Zhou, T., Zhan, X., Cui, H., 2018, Incorporation of Cesium Ions into $MA_{1-x}Cs_xPbI_3$ Single Crystals: Crystal Growth, Enhancement of Stability, and Optoelectronic Properties, *Journal of Physical Chemistry Letters*, Vol. 9, Hal. 5833–5839, DOI: 10.1021/acs.jpclett.8b02390.

Duan, M., Wang, Y., Zhang, P., Du, L., 2023, Effect of Cs^+ Doping on the Carrier Dynamics of $MAPbI_3$ Perovskite, *Materials*, Vol. 16, DOI: 10.3390/ma16176064.

Habisreutinger, S.N., McMeekin, D.P., Snaith, H.J., Nicholas, R.J., 2016, Research Update: Strategies for Improving the Stability of Perovskite Solar Cells, *APL Materials*, Vol. 4, DOI: 10.1063/1.4961210.

Han, F., Luo, J., Zhao, B., Wan, Z., Wang, R., Jia, C., 2017, Cesium Iodide Interface Modification for High Efficiency, High Stability and Low Hysteresis Perovskite Solar Cells, *Electrochimica Acta*, Vol. 236, DOI: 10.1016/j.electacta.2017.03.139.

Jiajia Zhang, 2024, Enhanced Phase Stability and Reduced Bandgap for $CsPbI_3$ Perovskite through Bi_3^+ and Cl^- Co-Doping, *Russian Journal of Physical Chemistry A*, Vol. 98, Hal. 2146–2151, DOI: 10.1134/S0036024424701279.

Roy, P., Ghosh, A., Barclay, F., Khare, A., Cuce, E., 2022, Perovskite Solar Cells: A Review of the Recent Advances, *Coatings*, Vol. 12, Hal. 1–24, DOI: 10.3390/coatings12081089.

Shahiduzzaman, M., Yonezawa, K., Yamamoto, K., Ripolles, T.S., Karakawa, M., Kuwabara, T., Takahashi, K., Hayase, S., Taima, T., 2017, Improved Reproducibility and Intercalation Control of Efficient Planar Inorganic Perovskite Solar Cells by Simple Alternate Vacuum Deposition of PbI_2 and CsI, *ACS Omega*, Vol. 2, Hal. 4464–4469, DOI: 10.1021/acsomega.7b00814.

Wang, L. Le, Shahiduzzaman, M., Muslih, E.Y., Nakano, M., Karakawa, M., Takahashi, K., Tomita, K., Nunzi, J.M., Taima, T., 2021, Double-Layer CsI Intercalation into an $MAPbI_3$ Framework for Efficient and Stable Perovskite Solar Cells, *Nano Energy*, Vol. 86, Hal. 106135, DOI: 10.1016/j.nanoen.2021.106135.

Wang, Q., Phung, N., Di Girolamo, D., Vivo, P., Abate, A., 2019, Enhancement in Llifespan of Halide Perovskite Solar Cells, *Energy and Environmental Science*, Vol. 12, Hal. 865–886, DOI: 10.1039/c8ee02852d.

Xiao, C., Zhang, F., Li, Z., Harvey, S.P., Chen, X., Wang, K., Jiang, C.S., Zhu, K., Al-Jassim, M., 2020, Inhomogeneous Doping of Perovskite Materials by Dopants from Hole-Transport Layer, *Matter*, Vol. 2, Hal. 261–272, DOI: 10.1016/j.matt.2019.10.005.

Zhang, P., Wu, J., Zhang, T., Wang, Y., Liu, D., Chen, H., Ji, L., Liu, C., Ahmad, W., Chen, Z.D., Li, S., 2018, Perovskite Solar Cells with ZnO Electron-Transporting Materials, *Advanced Materials*, Vol. 30, Hal. 1–20, DOI: 10.1002/adma.201703737.